

1D phased array for imaging applications in air utilizing MEMS ultrasonic transmitters

Marcel Jongmanns, Fraunhofer Institute for Photonic Microsystems (IPMS), Dresden, Germany, marcel.jongmanns@ipms.fraunhofer.de

Jorge Mario Monsalve, Fraunhofer Institute for Photonic Microsystems (IPMS), Dresden, Germany

Abstract

We designed a 1D ultrasonic array for phased array applications based on the lateral micromachined ultrasonic transducers (L-CMUT), which are in-house designed and manufactured at the Fraunhofer IPMS. The 1D array is a pretest for a 2D configuration, which would allow beam steering in 2 dimensions. The functionality of the 1D array and its control electronics have been tested and verified. Steering of the beam is possible in 0.33° steps in a range of $\pm 30^\circ$ before the amplitude decreases up to a maximum angle of $\pm 60^\circ$. To characterize the sound field, a setup utilizing an industrial cobot equipped with a reference microphone has been realized. To test the imaging capabilities different objects have been placed up to 1 m in front of the phased array. The measurement system can be used to detect the distance and position of an object relative to the position of the phased array.

1 Introduction

Phased arrays are commonly used for medical imaging, i.e. for measurements in water or soft tissue. Air-based ultrasonic imaging can be of interest to perform a presence detection or object tracking inside a room. It could also be used to increase the information acquired by parking sensors in cars, as it not only gives information about the distance, but also the incident angle; nonetheless, airborne ultrasound is often only used for distance measurements. One restriction that has usually limited the development of phased arrays in air is a transducer size below $\lambda/2$, where λ is the wavelength. A center-to-center distance below $\lambda/2$ is necessary to avoid so-called ‘grating lobes’: peaks in the radiation pattern that are comparable to the main lobe but lie at an undesired angle [1]. Bulk piezoelectric transducers usually have a membrane diameter above $\lambda/2$, although some methods exist to implement a phased array with them, such as external funnel structures [3] or spiral arrays [4] — both of which increase the size of the device significantly. MEMS components, such as capacitive MUTs (CMUTs) have been implemented for imaging purposes in air, although slightly trespassing the $\lambda/2$ limit [5]. A recent work has been published, where a MEMS microphone (which is naturally compact) is operated as a transmitter in a phased array [6], detecting objects in the centimeter range. Both the works in [5] and [6] achieve a range below 70 cm. With a lateral CMUT (L-CMUT), the concept of which we describe in [2], there is more flexibility for reducing the chip size below $\lambda/2$ without affecting neither its resonance frequency nor its bandwidth, only reducing the signal amplitude. In this work, we implement a one-dimensional array of L-CMUTs operating as transmitters and evaluate its performance.

2 Setup

A 1D array of 8 L-CMUT is mounted on a PCB as ultrasonic transmitter and 3 wideband MEMS microphones (Knowles SPH18C3LM4H-1) are used as receivers (Fig. 1). Each of the L-CMUT elements is 4 mm x 4 mm in size.

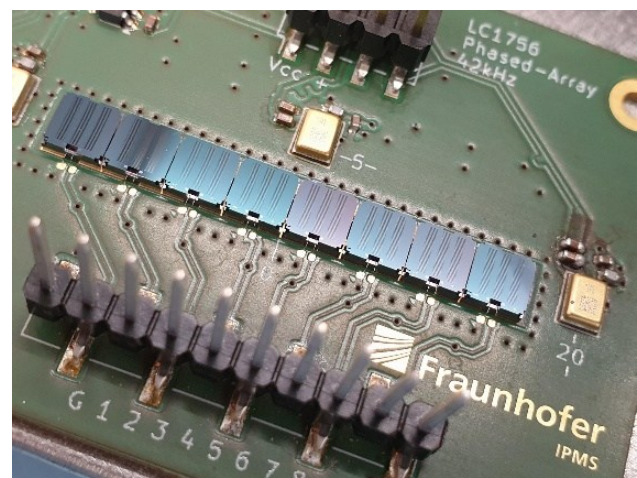


Figure 1: 1D-Array consisting of 8 L-CMUT elements and microphones as receiver.

The spacing between the center of the elements is 4.08 mm. This corresponds to a transmitting frequency of 42 kHz for phased array applications. Out of the 3 receivers only one is used in the later tests. It is in the middle of the array 5 mm (center of L-CMUT to center of acoustic port) above it. Knowing the spacing between consecutive elements (s) and the speed of sound (c), the time delay (Δt_m) that ought to be introduced the m th transducer ($m=0, 1, \dots, N-1$) in order to shift the main lobe by an angle ϕ can be calculated as follows [1]:

$$\Delta t_m = \begin{cases} m \frac{s}{c} \sin \phi, & \phi \geq 0 \\ (N - m - 1) \frac{s}{c} |\sin \phi|, & \phi < 0 \end{cases}$$

The control electronics consists of a boost converter, output drivers, input amplifiers and a STM32 Nucleo-G474RE development board to control the system. The system is supplied with 5V via USB, which is also used to communicate with a PC. The boost converter generates the required 30 V bias voltage for the L-CMUT. The phased array is controlled by 8 timers of the microcontroller. The 3.3 V output is amplified to 30 V as AC signal for the L-CMUT, resulting in a square wave from 15 V to 45 V to

drive the L-CMUT. The microphone output is amplified by a variable factor and filtered by a hardware low-pass filter as anti-aliasing filter before the analog data is sampled at 2 MHz by the microcontroller.

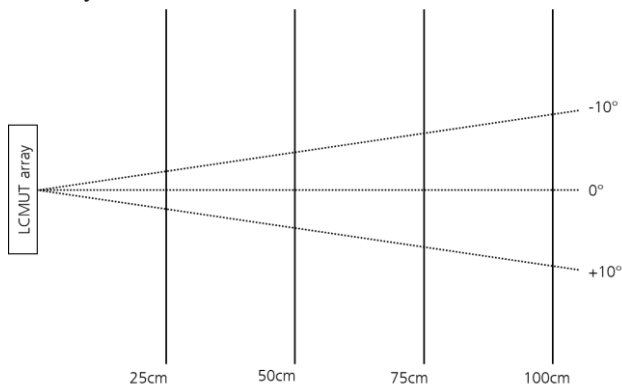


Figure 2: Schema of the field-of-view and object placement.

The laboratory test for object detection was performed on a table in a quiet office to reduce background noise. The 1D array was placed on one side of the table. Three different objects with different shapes were placed on the table. The objects were placed at 25 cm intervals from 25 cm to 125 cm apart from the measurement system (Fig. 2). For each object different angles relative to the system from -10° to $+10^\circ$ were tested. With this data the distance as well as the angle between the system and the object should be determined.

3 Characterization

To characterize the functionality of the phased array, a measurement setup was designed using a Universal Robots UR10 (Fig. 4). The sound pressure was measured using a calibrated GRAS 46DD 1/8" microphone, which was attached to the tool flange of the robotic arm. The UR10 was controlled by a PC running a Python script. This allowed the microphone to move in a hemisphere around the device under test while pointing the microphone at the device (Fig. 3). While this can be used to measure a 3D acoustic field, only a 2D measurement is shown. The measurement is performed along the center line along the length of the array in which the acoustic wave is steered. The angle θ describes the angle between the array and the perpendicular line, i.e. at $\theta = 0^\circ$ the acoustic beam travels straight on without steering. Transmitting, receiving and moving the robot was synchronized using the Python script.

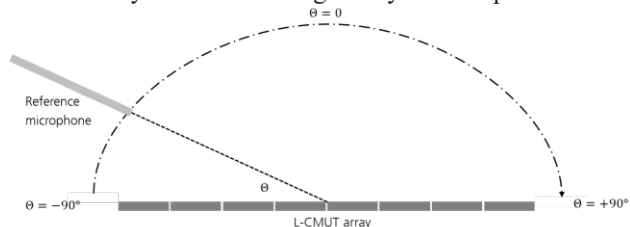


Figure 3: Schema of the movement of the reference microphone by the robot.

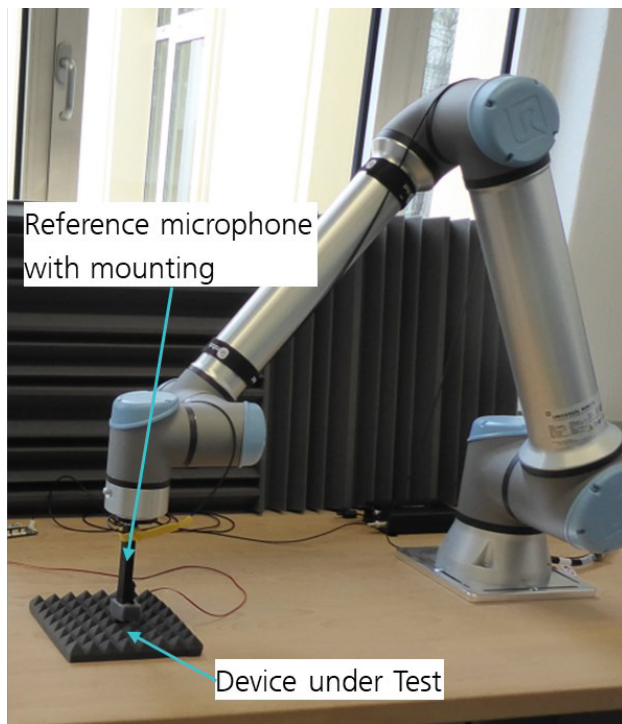


Figure 4: Actual measurement setup on the cobot.

4 Measurements

First, the array was characterized by the robotic measurement setup. The beam was steered from 0° to 90° in 5° steps. For each of these measurements the sound pressure was measured along the center line of the array in 1° steps in 10 cm distance (Fig. 5). From a steering angle of 0° to 25° , the amplitude is above 2 Pa. At 30° the amplitude falls below 2 Pa and diminishes further above 50° . Until 60° the set steering angle can be reached. At higher angles the side lobes become more prominent while the amplitude of the main beam is reduced even further, and the set steering angle cannot be reached anymore.

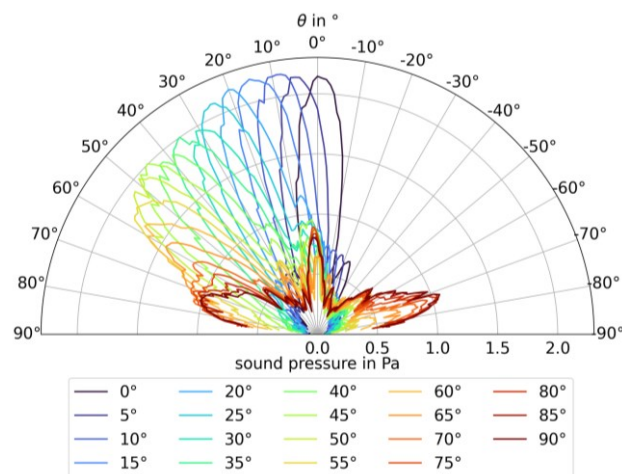


Figure 5: Measured sound pressures for different deflection angles.

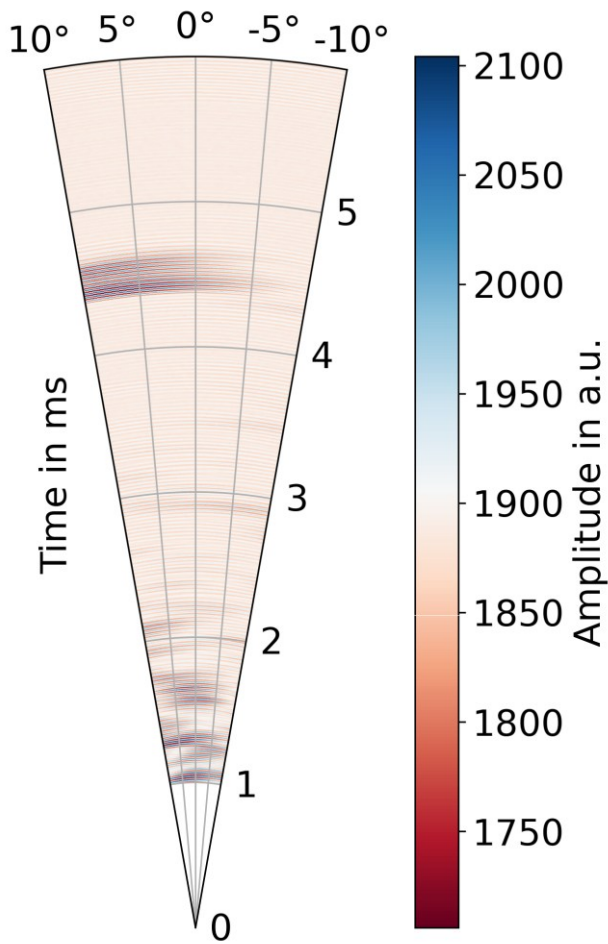


Figure 6: Line scan of an object placed 75 cm in front of the L-CMUT array at an angle of 5° .

As an example for object detection using a 1D line scan, a measurement of an object at 75 cm distance and an angle of 5° is shown in Fig. 6. The scan is performed with a steering angle from -10° to $+10^\circ$ in 0.33° steps. The first millisecond of the measurement has been omitted since it is governed by crosstalk. Even after that there is still a lot of noise caused by the table the system is on, the wall of the room and other objects in vicinity. However, there is also a peak in signal amplitude around 4.5 ms time-of-flight. At 75 cm distance, the total distance for a pulse-echo measurement is 150 cm. At room temperature the expected time-of-flight is $tof = \frac{1.5m}{343\frac{m}{s}} = 0.00437ms$, with the speed of sound 343m/s. This correlates well with the observed value.

Overall three different objects have been used for the scan. One was a box with a rectangular shape, one container with rectangular shape but rounded corners and one circular bottle. Looking closely at the reflected echo, one can see differences in the signal (Fig. 7). The box with sharp corners also shows a sharp difference between high and low amplitude in the reflection. The rounded corners and circular shape introduce phase shifts in the signal as well as a change in the amplitude of the reflected signal. This suggests that it is possible to not only detect the distance and position of an object, but also the shape.

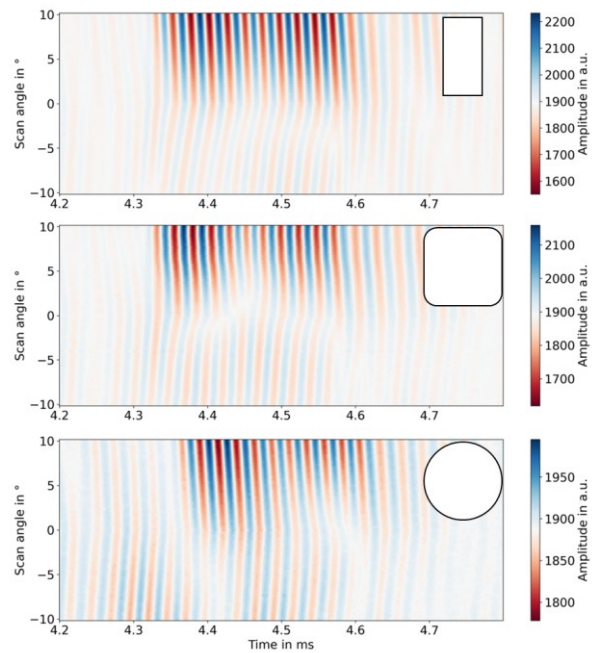


Figure 7: Reflection pattern of the scan of different object placed at 10° and 75 cm distance. Top: rectangular with sharp corners; Middle: rectangular with rounded corners; Bottom: circular.

One disadvantage of the line scan is the long measurement time. At 9 ms maximum time-of-flight, the maximum distance is around 3 m, or 1.5 m distance between measurement system and object. With a fine scan from -10° to $+10^\circ$ in 0.33° steps it requires 61 consecutive measurements for one image, which is overall 0.55s, excluding overhead to transfer the data from the system to the PC for further processing. A way to get around this restriction is to utilize different measurement approaches. Another tested approach tries to encode angular information by sending signals with different frequencies. As the L-CMUT is a wide-band transmitter, the same setup can be used to make a pulse-echo measurement where transmitter 1 sends a burst of 15 pulses at 40kHz, transmitter 5 at 50kHz and transmitter 8 at 60kHz. Transmitters 1 and 8 are the outermost and 5 is one of the middle transmitters. The distance between the transmitters is known from the design and the distance to an object can be calculated from the time-of-flight. This information can be used to calculate the distance and angle using the law of sines. Fig. 8 shows the measured signal, which has been treated with 3 different digital bandpass filters to retrieve each of the 3 different transmitter signals.

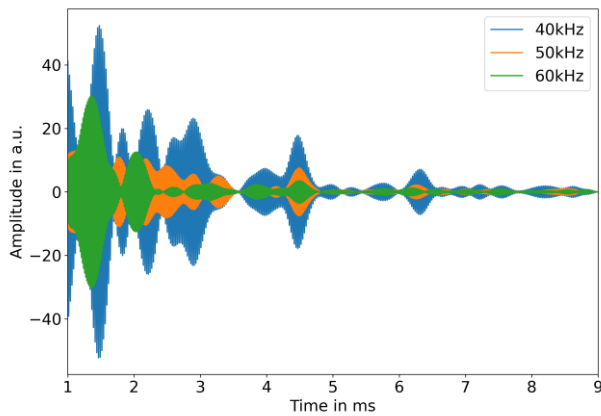


Figure 8: Decomposed signals of one multi-frequency measurement.

5 Discussion and outlook

A 1D phased array for ultrasonic line scans has been realized using L-CMUT wideband ultrasound transmitters. A custom driver electronic is used to control the system. The function of the system has been validated by making measurements of the acoustic field by an automated, robotic measurement setup.

Preliminary measurements utilizing a fine-pitched line scan with 0.33° resolution have been performed. Different objects have been placed at distances up to 1 m in front of the array and at different angles, which can be seen in the measured data. However, the system still suffers from crosstalk, which introduces a minimum distance to the object of about 50 cm. Ranges up to 1.25 m could be measured with this system during the laboratory tests, surpassing previous developments of in-air ultrasonic phased arrays. A new revision of the L-CMUT is currently being manufactured, which can be driven at higher voltages. This should increase the distance above 3m in a pulse-echo configuration.

A more extensive evaluation of possible algorithms for data processing is still open. While established algorithms like peak detection or correlation are easy to implement, they are susceptible to the crosstalk or static objects near the transmitter. One possibility is that the signal is normalized by removing static noise and only detect changes in the system. This would allow the system to detect moving objects for e.g. presence detection. Another planned approach is to utilize and evaluate AI-based algorithms, which could be used to detect different patterns in the ultrasonic signal and correlate them to different shapes of the object.

6 Acknowledgements

This work is co-funded by the German Federal Ministry of Research, Technology and Space in the project iCampus 2 (No. 16ME0420K). The authors like to thank Andreas Mrosk and Sven Püschel for support with the acoustical measurements and wire bonding of the MEMS devices.

7 Literature

- [1] L. W. Schmerr Jr, *Fundamentals of Ultrasonic Phased Arrays*, Springer, 2015
- [2] J. M. Monsalve, A. Melnikov, M. Stolz, A. Mrosk, M. Jongmanns, F. Wall, S. Langa, I. Marica-Bercu, T. Brändel, M. Kircher, H. A. G. Schenk, B. Kaiser, H. Schenk, "Proof of concept of an air-coupled electrostatic ultrasonic transducer based on lateral motion", *Sensors and Actuators A: Physical*, vol. 345, no. 113813, 2022, doi: 10.1016/j.sna.2022.113813
- [3] G. Allevato, J. Hinrichs, D. Grosskurth, M. Rutsch, J. Adler, A. Jäger, M. Pesavento, M. Kupnik, "3D imaging method for an air-coupled 40 kHz ultrasound phased-array", in *Proceedings of the 23rd International Congress on Acoustics*, 2019, pp. 4797-4804
- [4] G. Allevato et al., "Air-Coupled Ultrasonic Spiral Phased Array for High-Precision Beamforming and Imaging," in *IEEE Open Journal of Ultrasonics, Ferroelectrics, and Frequency Control*, vol. 2, pp. 40-54, 2022, doi: 10.1109/OJUFFC.2022.3142710
- [5] K. K. Park, B. T. Khuri-Yakub, "3-D airborne ultrasound synthetic aperture imaging based on capacitive micromachined ultrasonic transducers", *Ultrasonics*, vol. 53, pp. 1355-1362, 2013, doi: 10.1016/j.ultras.2013.04.003
- [6] S. Anzinger et al., "Low Power Capacitive Ultrasonic Transceiver Array for Airborne Object Detection," 2020 *IEEE 33rd International Conference on Micro Electro Mechanical Systems (MEMS)*, Vancouver, BC, Canada, 2020, pp. 853-856, doi: 10.1109/MEMS46641.2020.9056182